

# Prognostic role of CD11b<sup>+</sup> myeloid-derived suppressor cells in oral squamous cell carcinoma

Yue Jiang<sup>1</sup>, Chenxing Wang<sup>1</sup>, Yanling Wang<sup>1,2</sup>, Wei Zhang<sup>3</sup>, Laikui Liu<sup>3</sup>, Jie Cheng<sup>1,2</sup>

<sup>1</sup>Jiangsu Key Laboratory of Oral Disease, Nanjing Medical University, Jiangsu, China

<sup>2</sup>Department of Oral and Maxillofacial Surgery, Affiliated Stomatological Hospital, Nanjing Medical University, Nanjing, China

<sup>3</sup>Department of Oral Pathology, Affiliated Stomatological Hospital, Nanjing Medical University, Nanjing, China

**Submitted:** 2 August 2019; **Accepted:** 19 January 2020

**Online publication:** 25 March 2021

Arch Med Sci 2023; 19 (1): 171–179

DOI: <https://doi.org/10.5114/aoms/116683>

Copyright © 2021 Termedia & Banach

## Corresponding author:

Jie Cheng DDS, PhD,  
Assoc. Prof.

Department of Oral  
and Maxillofacial Surgery  
Affiliated Stomatological  
Hospital

Nanjing Medical University  
136 Hanzhong Road

Nanjing, Jiangsu  
Province, China

Phone: +86-25-85031880

E-mail: [jie\\_cheng\\_njnu@163.com](mailto:jie_cheng_njnu@163.com)

## Abstract

**Introduction:** Myeloid-derived suppressor cells (MDSCs) are critically involved in cancer immune suppression and MDSC density has been recognized as a robust prognostic biomarker. Here, we sought to characterize the densities and locations of CD11b<sup>+</sup> MDSCs in primary oral squamous cell carcinoma (OSCC) and determine their prognostic significance.

**Material and methods:** A total of 144 eligible OSCC samples from a tertiary referral oral cancer center were retrospectively collected. Intensities of CD11b<sup>+</sup> MDSCs at the tumor center (CT) and invasive margin (IM) in OSCC samples were detected by immunohistochemistry and automatically quantified using Image J software. The optimal cutoff values for CD11b CT and CD11b IM were determined by X-tile based on overall survival. The associations between CD11b<sup>+</sup> MDSCs and clinicopathological parameters were assessed by the  $\chi^2$  test. The prognostic value of CD11b<sup>+</sup> MDSCs was evaluated by Kaplan-Meier plots, Cox regression analyses and receiver operating characteristics curves.

**Results:** High density of CD11b<sup>+</sup> MDSCs at CT or IM was significantly associated with inferior overall and disease-free survival (Kaplan-Meier,  $p < 0.05$ , log-rank test). CD11b CT and CD11b IM were identified as independent prognostic predictors for patient survival. The prediction accuracy and specificity of CD11b CT and CD11b IM were superior to other prognostic parameters.

**Conclusions:** Our data indicated that increased densities of CD11b<sup>+</sup> MDSCs in CT and IM regions were significantly associated with poor prognoses, which might be novel prognostic factors for OSCC.

**Key words:** oral squamous cell carcinoma, myeloid derived suppressor cells, CD11b, prognostic biomarker.

## Introduction

The 5-year survival for patients with primary oral squamous cell carcinoma (OSCC) remains at approximately 60%, which has not been markedly improved in the past decades [1]. Such a dismal prognosis is in part due to the high proportion of patients who present with advanced disease at the initial diagnosis. Insufficient and inaccurate evaluation of this malignancy hampers effective treatment planning and proper prognostic prediction. Nowadays, patients with OSCC are commonly staged according to the TNM staging system based on the tumor dimension,

lymph node and metastasis [2]. However, owing to the heterogeneity of OSCC, patients with the same TNM stage usually present a significant variety of clinical outcomes [3]. Thus, identification of novel prognostic factors is urgently needed to better estimate survival and guide treatment planning.

The tumor microenvironment of solid cancer including OSCC is usually characterized by significant infiltration of both innate and adaptive immune cells including but not restricted to T cells, B cells and macrophages [4]. Mounting evidence has demonstrated that various types of tumor-infiltrating immune cells promote cancer initiation, overgrowth and metastatic dissemination [5]. Moreover, quantifications of these cancer-associated immune cells have robust prognostic significance in a broad spectrum of human cancer [6]. In particular, myeloid-derived suppressor cells (MDSCs), one of the major components of the tumor microenvironment, have emerged as a key regulatory cell population that critically participates in tumorigenesis [7]. Intensive studies have indicated MDSCs as a negative predictor of clinical outcomes in various cancers and a potential predictive biomarker in malignancies including melanoma, gastrointestinal and bladder cancer [8–10]. Currently, human MDSCs are usually labelled as CD11b<sup>+</sup>CD33<sup>+</sup>HLA-DR<sup>-</sup>Lin<sup>-</sup> and consist of two groups of cells termed polymorphonuclear (PMN-MDSCs, CD11b<sup>+</sup>CD33<sup>+</sup>CD14<sup>-</sup>CD15<sup>+</sup>HLA-DR<sup>-</sup>Lin<sup>-</sup>) and monocytic (M-MDSCs, CD11b<sup>+</sup>CD33<sup>+</sup>CD14<sup>+</sup>CD15<sup>-</sup>HLA-DR<sup>-</sup>Lin<sup>-</sup>) [11]. Several previous studies have used the CD11b to label tumor-infiltrating MDSCs by immunohistochemistry in various cancer contexts. Evaluation of CD11b<sup>+</sup> MDSCs in the tumor center and microenvironment has been utilized to predict patients' clinical outcome [11, 12]. For example, high densities of CD11b<sup>+</sup> MDSCs were significantly associated with unfavorable survival of patients diagnosed with hepatocellular carcinoma [13]. However, to the best of our knowledge, the prognostic value of CD11b<sup>+</sup> MDSCs infiltration in OSCC remains largely unknown.

The present study was designed to evaluate the densities of CD11b<sup>+</sup> MDSCs in both center of tumor (CT) and invasive margin (IM) regions by immunohistochemistry and assess their prognostic significance in a retrospective cohort of OSCC from a tertiary referral oral cancer center.

## Material and methods

### Patients and specimens

This study was in accordance with the Declaration of Helsinki and approved by the Research Ethic Committees of Affiliated Stomatological Hospital, Nanjing Medical University. Informed

consent was obtained from each patient or their guardians. Records of patients with primary OSCC who underwent ablative surgery at the Affiliated Stomatological Hospital of Nanjing Medical University between April 2011 and December 2013 were reviewed. Patients enrolled here suffered from primary OSCC and were treatment-naive. Formalin-fixed paraffin-embedded (FFPE) specimens from ablative resection of OSCC and detailed clinical, pathological as well as follow-up data were available for all eligible patients. Histo-pathological grading and clinical staging of each case were evaluated according to the WHO classification and American Joint Committee on Cancer Staging System 7<sup>th</sup> edition, respectively [14].

### Immunohistochemical staining of CD11b in OSCC

The FFPE specimens of all patients enrolled were collected for slide preparation. Immunohistochemical staining of CD11b was performed on 4- $\mu$ m thickness sections as described previously [15]. Briefly, FFPE specimens were consecutively sliced into sections followed by deparaffinization in xylene and standard gradient ethanol. Subsequently, the slides were immersed in Tris-EDTA buffer (pH 8.0) for 15 min for antigen retrieval and incubated in 3% H<sub>2</sub>O<sub>2</sub> for the blockage of endogenous peroxidase activity. The sections were further incubated with primary antibody (anti-CD11b, 1 : 200 dilution, CST, 49420) at 4°C overnight followed by phosphate-buffered saline washing and biotinylated secondary antibody incubation (Maxim, China). Finally, the antigen detection was conducted by a color reaction with 3,3-diaminobenzidine (DAB) under microscopic monitoring and counterstained with hematoxylin. Negative controls without primary antibody incubation were included.

### Evaluation of immunohistochemical staining

Images of selected areas were acquired using an upright microscope (Leica DM4000B, Germany), and the immunohistochemical staining results of CD11b<sup>+</sup> MDSCs in OSCC samples were independently assessed by two senior oral pathologists without knowledge of patients' clinicopathological data. When an agreement was difficult to reach, the final judgment was made by reevaluating the slides. For each tumor specimen, slides containing invasive margin (IM) and tumor center (CT) regions were selected. Five representative fields per slide including both of the regions were selected at 200 $\times$  magnification after initial screening under a low power field (100 $\times$ ). As illustrated in Figure 1, similar to previous reports, the invasive margin (IM) was defined as a region of

500  $\mu\text{m}$  width on each side of the border between malignant cells and tumor stroma, while the tumor center (CT) was defined as a region in the center of the tumor which was full of malignant cells and excluded the first 250  $\mu\text{m}$  adjacent to the tumor border [16, 17]. The density of CD11b<sup>+</sup> MDSCs in OSCC specimens was recorded independently at the CT and IM and presented as the mean number of positively stained cells per  $\text{mm}^2$ , similar to our previous report [18–20]. As shown in Figure 2, cell counts of CD11b<sup>+</sup> MDSCs were automatically quantified using ImageJ (version 2.0). The optimal cut-off values for the densities of CD11b<sup>+</sup> MDSCs at the CT and IM were determined after analyzing the association between cell amount and overall survival (OS) by X-tile software with a minimum *p*-value approach (version 3.6.1, <https://medicine.yale.edu/lab/rimm/research/software/>). The X-tile program is a commonly used statistical tool for the assessment of biological relationships between a biomarker and outcome and identification of the optimal cut-point based on marker expression [21].

### Statistical analysis

The X-tile program was applied to determine the optimal cut-off value of the CD11b<sup>+</sup> MDSC density with the minimum *p*-value. Analysis of the association between classified densities of CD11b<sup>+</sup> MDSCs at CT or IM and multiple clinicopathological parameters was conducted using the  $\chi^2$  test or Fisher's exact test. Overall survival (OS) and disease-free survival (DFS) were calculated with the Kaplan-Meier method and comparison

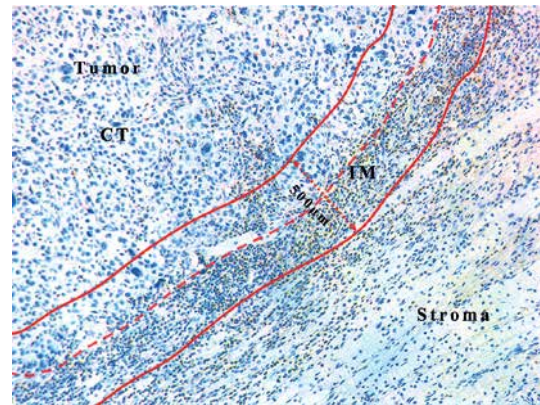


**Figure 1.** Representative IHC image of CD11b<sup>+</sup> MDSCs in OSCC. The dotted red line marks the border between the tumor and the surrounding stroma. Two red lines mark a region (IM) 500  $\mu\text{m}$  wide (dotted red line with arrow) on each side of the border between malignant cells and the surrounding nontumor stroma. CT comprised the tumor section excluding the first 250  $\mu\text{m}$  adjacent to the tumor border

between groups was performed with the log-rank test. Univariate and multivariate Cox proportional hazards regression models were used to determine the hazard ratio of different prognostic factors and the association between these factors with OS and DFS for OSCC. Receiver operating characteristics (ROC) curves of indicated prognostic factors were plotted and the area under the curve (AUC) was calculated to identify the predictive performance of each individual marker. All tests were two-sided, and *p*-values less than 0.05 were considered statistically significant. All statis-

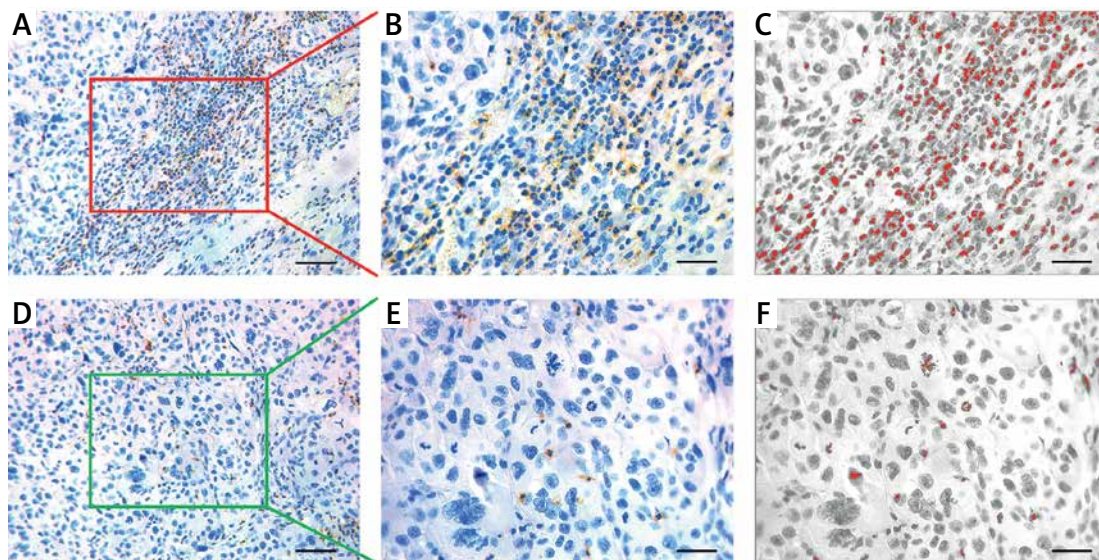


**Figure 2.** Immunohistochemical staining of CD11b<sup>+</sup> MDSCs in OSCC. **A** – Representative staining of CD11b<sup>+</sup> MDSCs in the tumor center (CT) of OSCC. Scale bar: 100  $\mu\text{m}$ . **B, C** – The number of CD11b<sup>+</sup> MDSCs in tumor CT is semi-automatically quantified by ImageJ software. Scale bar: 50  $\mu\text{m}$ . **D** – Representative staining of CD11b<sup>+</sup> MDSCs in invasive margins (IM) of OSCC. Scale bar: 100  $\mu\text{m}$ . **E, F** – The number of CD11b<sup>+</sup> MDSCs in tumor IM is semi-automatically quantified by ImageJ software. Scale bar: 50  $\mu\text{m}$

tical analysis was performed with GraphPad Prism 8.0, IBM SPSS 22.0 software and R 3.5.3.

## Results

### Epidemiological and clinicopathological characteristics of patients

One hundred and forty-four patients (76 males and 68 females) who were diagnosed with primary OSCC and underwent ablative surgery were included. They were aged from 30 to 82 years. The median follow-up duration was 45 months (ranging from 6 to 138 month). Sixty-nine patients died during the follow-up and 8 patients with local recurrence or cervical node metastasis remained alive until the last follow-up. Detailed epidemiological and clinicopathological characteristics of these patients enrolled are summarized in Table I.

### Associations between infiltrating CD11b+ MDSCs and clinicopathological features

Here, we employed immunochemical staining of CD11b, a common marker to label MDSCs in cancer, to characterize and quantify MDSCs in primary OSCC [7, 11, 12]. As shown in Figure 2, CD11b positive staining MDSCs was readily detected in CT and IM regions in OSCC samples. Following image capture and automatic cell counting by ImageJ, the densities of CD11b+ MDSCs in each tumor region (CT, IM) was calculated and recorded

(Figure 2). Our results revealed that the densities of infiltrating MDSCs varied in CT ( $130.9 \pm 5.84$  per  $\text{mm}^2$ ) and IM ( $466.2 \pm 15.28$  per  $\text{mm}^2$ ), thus suggesting the significant enrichment of MDSCs in IM compartments. Additionally, no significant association between intensities of CD11b+ MDSCs in CT and IM was identified (data not shown). Then, to achieve outcome-based cut-off optimization, the “minimum *p*-value” approach was employed using X-tile software [21]. The optimal cutoff value for CD11b+ MDSC at the IM was 389.0 per  $\text{mm}^2$  ( $p = 0.0012$ ) and 143.0 per  $\text{mm}^2$  at the CT ( $p = 0.00189$ ) (Figure 3). Consequently, patients were classified into low or high CD11b+ MDSC subgroups. As summarized in Table I, we analyzed the associations between CD11b+ MDSC densities and several clinicopathological parameters, but failed to identify any significant associations.

### Association between infiltrating CD11b+ MDSCs and survival in OSCC patients

To identify the possible associations between CD11b+ MDSCs and patient survival, we performed Kaplan-Meier analyses and found that increased densities of CD11b+ MDSCs in both CT and IM regions were significantly associated with shorter OS and DFS (Figures 4 A–D). Furthermore, we verified the prognostic values of these immunological features for OSCC by Cox regression analysis. As shown in Table II, the univariate anal-

**Table I.** Associations between density of CD11b+ MDSCs and clinicopathological parameters in OSCC

Variable	CD11b CT			CD11b IM		
	$\geq 143.0$	$< 143.0$	<i>P</i> -value*	$\geq 389.0$	$< 389.0$	<i>P</i> -value*
No. of patients	54	90		89	55	
Age [years]	$\leq 60$	18	0.8905	24	23	0.0648
	$> 60$	36		65	32	
Gender	Male	31	0.3887	49	27	0.4860
	Female	23		40	28	
Smoking	No	39	0.2142	69	42	0.8717
	Yes	15		20	13	
Alcohol use	No	45	0.7197	76	46	0.7759
	Yes	9		13	9	
Tumor size	T1-T2	42	0.4083	73	44	0.7626
	T3-T4	12		16	11	
Pathological grade	I	46	0.1101	78	52	0.2493
	II–III	8		11	3	
Cervical node metastasis	N0	38	0.4741	60	41	0.3637
	N+	16		29	14	
Clinical stage	I–II	28	0.2217	50	34	0.5049
	III–IV	26		39	21	

\*All *p*-values in Table I were obtained using  $\chi^2$  test or Fisher's exact test. MDSCs – myeloid derived suppressor cells, OSCC – oral squamous cell carcinoma, CT – tumor center, IM – invasive margin.

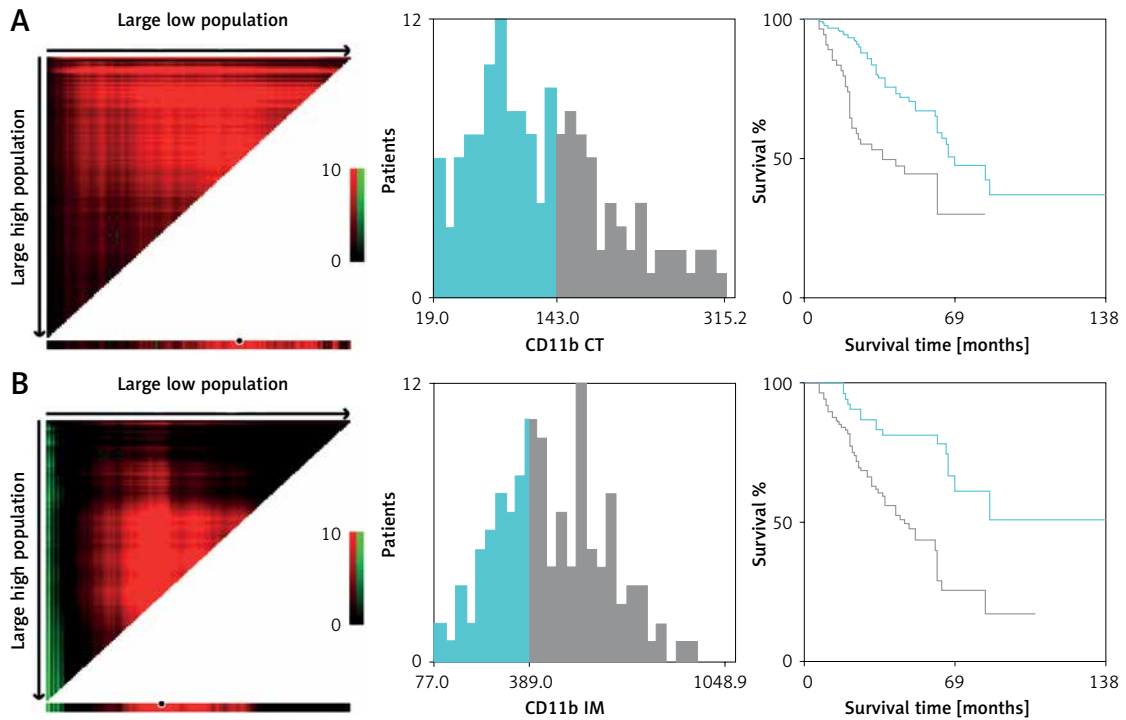


**Figure 3.** Optimal cutoff values of CD11b<sup>+</sup> MDSCs in the CT (A) and IM (B) were determined by X-tile software using OS as the primary outcome in our patient cohort  
 CT – tumor center, IM – invasive margin.

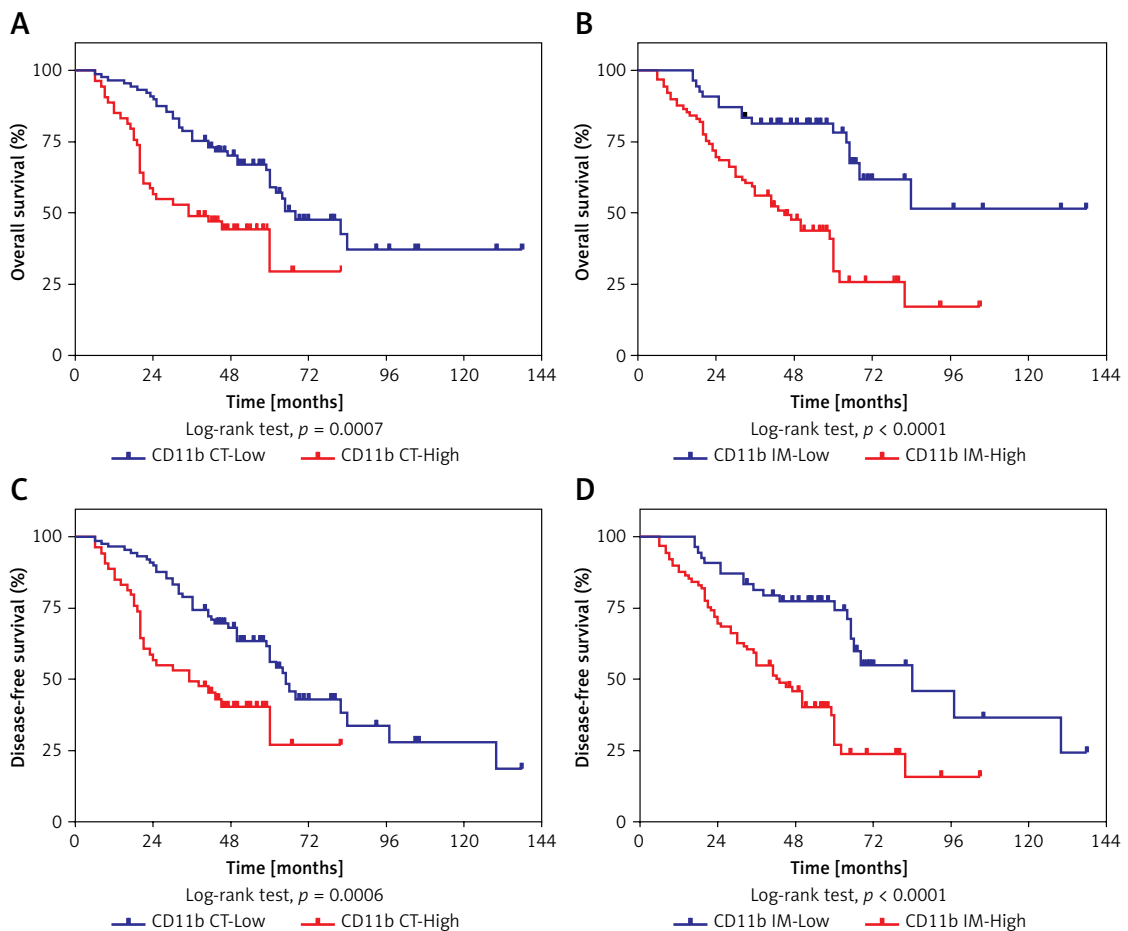


**Figure 4.** Prognostic significance of CD11b CT and CD11b IM in patients with OSCC. Kaplan-Meier analysis of overall survival (OS) and disease-free survival (DFS) in patients stratified by CD11b CT (A, C) and CD11b IM (B, D).  $P$ -values were calculated with the log-rank test

**Table II.** Univariate and multivariate survival analyses of prognostic factors associated with OS and DFS for OSCC

Variables	OS			DFS		
	HR	95% CI	P-value	HR	95% CI	P-value
Univariate survival analyses:						
Age (> 60, ≤ 60)	0.893	0.546–1.461	0.653	1.028	0.639–1.654	0.909
Gender (male, female)	0.812	0.505–1.306	0.391	0.816	0.520–1.280	0.376
Smoking (yes, no)	0.749	0.402–1.397	0.363	0.807	0.451–1.442	0.469
Alcohol use (yes, no)	1.163	0.610–2.217	0.647	1.280	0.704–2.328	0.419
Tumor size (T3-T4, T1-T2)	1.264	0.712–2.243	0.424	1.329	0.773–2.286	0.303
Pathological grade (II-III, I)	1.942	0.958–3.938	0.066	2.496	1.338–4.658	0.004
Cervical node metastasis (N+, N0)	0.993	0.583–1.692	0.981	1.086	0.658–1.793	0.746
Clinical stage (III-IV, I-II)	1.217	0.749–1.978	0.427	1.395	0.879–2.215	0.158
CD11b CT (high, low)	2.283	1.390–3.750	0.001	2.235	1.388–3.597	0.001
CD11b IM (high, low)	3.285	1.850–5.835	< 0.001	2.868	1.693–4.857	< 0.001
Multivariate survival analyses:						
Pathological grade (II-III, I)	1.643	0.774–3.487	0.196	2.171	(1.105–4.265)	0.024
Cervical node metastasis (N+, N0)	0.599	0.269–1.332	0.209	0.536	(0.255–1.128)	0.101
Clinical stage (III-IV, I-II)	1.542	0.760–3.130	0.230	1.836	(0.949–3.552)	0.071
CD11b CT (high, low)	2.012	1.213–3.337	0.007	1.919	(1.181–3.119)	0.009
CD11b IM (high, low)	3.183	1.780–5.689	< 0.001	2.762	(1.618–4.715)	< 0.001

Numbers in bold indicate statistical significance with p-values less than 0.05. HR – hazard ratio, CI – confidence interval, OS – overall survival, DFS – disease-free survival, OSCC – oral squamous cell carcinoma, CT – tumor center, IM – invasive margin.

ysis indicated that elevated densities of CD11b<sup>+</sup> MDSCs at either the IM or CT were significantly associated with reduced OS ( $p = 0.001$  and  $< 0.001$ , respectively) and DFS ( $p = 0.001$  and  $< 0.001$ , respectively). Moreover, the multivariate Cox proportional regression analyses revealed that, besides pathological grade, densities of CD11b<sup>+</sup> MDSCs

in the IM or CT were independent prognostic factors for OS (HR = 3.183, 95% CI: 1.780–5.689,  $p < 0.001$  at IM; HR = 2.012, 95% CI: 1.213–3.337,  $p = 0.007$  at CT). Similar results were found in the DFS analysis, where estimated HR for CD11b<sup>+</sup>MDSCs in the IM was 2.762 (95% CI: 1.618–4.715) and at the CT was 1.919 (95% CI: 1.181–3.119).

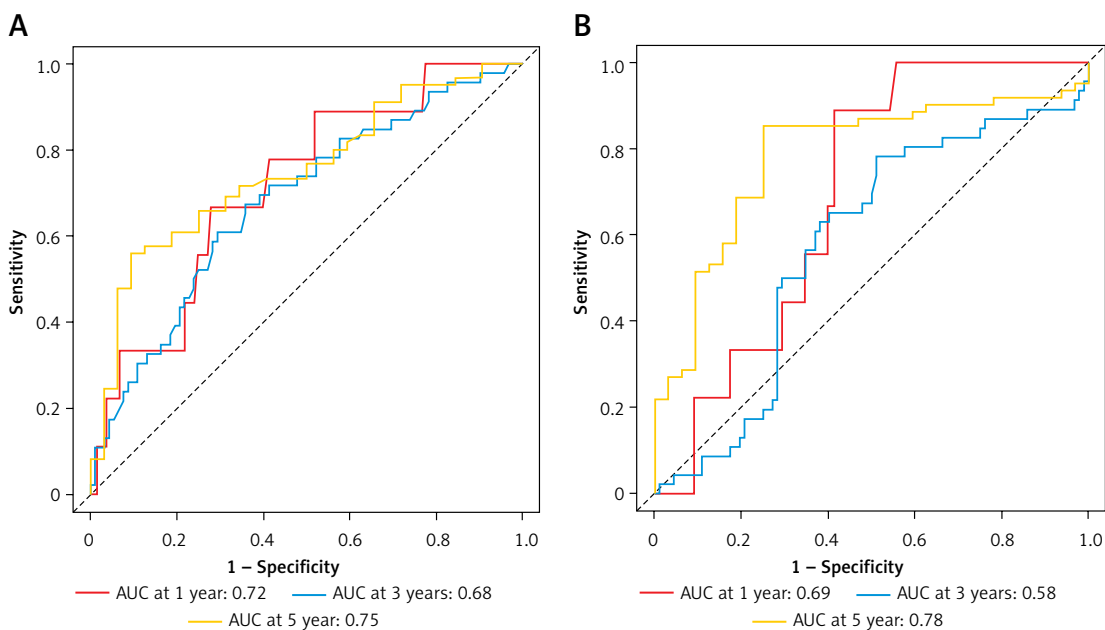


**Figure 5.** Predictive ability of CD11b CT and CD11b IM for the prognosis of patients with OSCC. ROC curves and AUC at 1 year, 3 years and 5 years were used to estimate the sensitivity and specificity of CD11b CT (A) and CD11b IM (B) in the prognostic prediction of overall survival (OS)

### Predictive performance of CD11b<sup>+</sup> MDSCs for OSCC prognosis

Next, we proceeded to determine the predictive performance of CD11b<sup>+</sup> MDSCs for patients with OSCC by time-dependent ROC curve analysis. Tumor size, cervical nodal metastasis, pathological grade and clinical stage, widely adopted as prognostic factors for OSCC, were included for assessing the predictive value of CD11b<sup>+</sup> MDSCs. With respect to the OS, the AUC values of CD11b IM at 1 year, 3 years and 5 years were 0.69, 0.58, 0.78 and the AUC values of CD11b CT were 0.72, 0.68, 0.75, respectively (Figure 5 A, B). However, the AUC of the aforementioned four clinicopathological parameters was less than 0.54 (Figure 6).

### Discussion

High mortality in OSCC necessitates development of effective biomarkers for treatment planning and prognostic prediction, ultimately improving patient management and long-term survival. The current commonly used TNM staging system fails to meet the clinical demand in accurate prognostic prediction [1]. Although various genetic or epigenetic biomarkers in OSCC have been proposed for prognostic assessment including microRNA, lncRNA and alternative mRNA splicing signature, they are still far from optimal [20, 22, 23]. In addition to these intrinsic features of cancer itself, tumor-infiltrating immunocytes have been established as key drivers underlying tumorigenesis as well as novel biomarkers with tremendous diagnostic and prognostic significance [4, 6]. Here, we determined the location and amount of MDSCs in OSCC and revealed that a high amount of CD11b<sup>+</sup> MDSCs was associated with inferior survival and quantification of CD11b<sup>+</sup> MDSCs might be a novel independent prognostic factor for OSCC.

Accumulating evidence has demonstrated that multiple types of immune cells infiltrate in the tumor itself or its microenvironment facilitate tumor overgrowth, invasion and metastasis [5]. In particular, MDSCs are a heterogeneous population of immature myeloid cells and utilize multiple mechanisms to establish a tumor-promoting environment [7, 11]. They can suppress T cells by depleting amino acids necessary for activation of T cells, inhibiting their migration and preventing their entry into lymph nodes or homing to tumor sites [24, 25]. Moreover, with respect to their indirect immunosuppressive mechanism, MDSCs altered the ability of antigen-presenting cells (APCs) to activate T cells and T regulatory cells (Tregs) [26]. Besides immune regulatory mechanisms, MDSCs also influenced tumor progression by modulating the tumor microenvironment and promoting angiogenesis via VEGF, bFGF and MMP9 [27, 28].

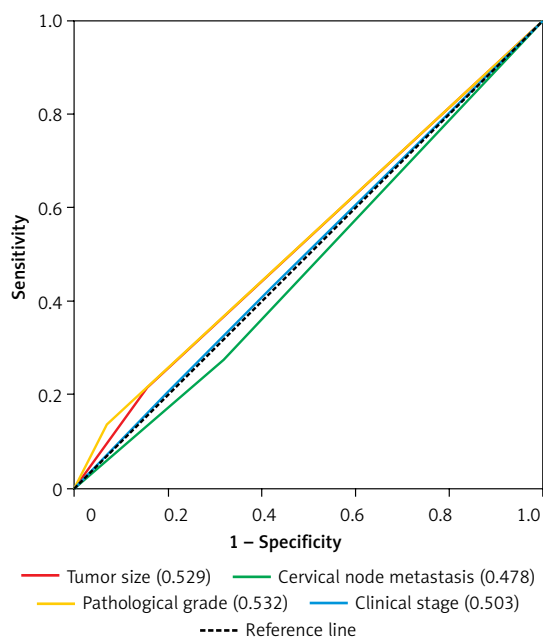


**Figure 6.** Predictive ability of tumor size, cervical node metastasis, pathological grade and clinical stage for the prognosis of patients with OSCC. The sensitivity and specificity of four clinicopathological parameters in the prognostic prediction of overall survival (OS) were estimated by ROC curves

Consistent with these previous findings, our data revealed that MDSCs were highly enriched in invasive tumor margins, thus suggesting that their tumor-promoting roles occurred primarily in the tumor microenvironment. However, much work is needed to accurately dissect the roles of MDSCs and relevant mechanisms of action during OSCC tumorigenesis.

Until now, the prognostic impacts of several subsets of tumor-infiltrating immune cells in a broad spectrum of human cancers including OSCC have been documented, such as CD3<sup>+</sup> TIL, CD8<sup>+</sup> TIL, CD45RO<sup>+</sup> TIL and CD11b<sup>+</sup> MDSCs [12, 18, 19, 29]. For example, we reported that high densities of CD3<sup>+</sup>/CD8<sup>+</sup> TIL and CD68<sup>+</sup> macrophage were significantly associated with increased overall and disease-specific survival in OSCC [19, 30]. In the present study, we assessed the prognostic value of the density of CD11b<sup>+</sup> MDSCs in either CT or IM regions. Our results revealed that high densities of CD11b<sup>+</sup> MDSCs were significantly associated with reduced patient survival. In addition, multivariate Cox regression assay also identified CD11b<sup>+</sup> MDSCs as a novel independent prognostic factor affecting patient survival. These findings are in line with previous reports wherein MDSC accumulation correlated with poor outcome in melanoma, gastrointestinal cancers and bladder cancer [8–10, 31]. Moreover, MDSCs in non-small lung and cervical cancer patients were associated with advanced tumor stage and unfavorable prognosis and served as an independent prognostic factor

predicting patients' outcome [32, 33]. Here, we investigated the prognostic value of CD11b<sup>+</sup> MDSCs in distinct locations (CT or IM) in OSCC with a relatively long-term follow-up. Our findings revealed that high densities of CD11b<sup>+</sup> MDSCs in either the IM or CT compartment were significantly associated with unfavorable prognosis in OSCC and also served as independent prognostic factors in predicting patients' survival. Previous studies mainly focused on MDSCs in whole tumor sections without discriminating different locations of infiltrating immunosuppressive cells in the tumor sample, which may partially explain the inconsistent results among various studies [10, 31–33]. Indeed, spatial distribution of immunoregulatory cells in different compartments such as the CT and IM might have diverse biological functions and their predictive value for clinical outcome may be region-specific [34]. Thus, we believe that our immunological evaluation of CD11b<sup>+</sup> MDSCs by taking their distribution into account might be more accurate and powerful. In support of this, our time-dependent ROC curve analysis also revealed that the predictive performance of CD11b<sup>+</sup> MDSCs in the IM or CT was superior to such prognostic factors as tumor size, cervical nodal metastasis and pathological grade.

Although our data revealed the prognostic values of CD11b<sup>+</sup> MDSCs in IM or CT for OSCC patients, there are some limitations. Firstly, potential bias may remain due to the retrospective nature and limited sample size. Our findings need to be confirmed in a prospective study including a large, multicenter patient population. A single marker for MDSC labeling might not be adequate to evaluate their diverse subtypes as well as functional status. Combinations of two or more markers might be better and more accurate to dissect the clinical and biological significance of MDSCs during OSCC initiation and progression. In addition, some pathological factors such as depth of invasion, extracapsular extension or perineural invasion were not included in the prognostic analyses. Furthermore, whether CD11b<sup>+</sup> MDSCs in IM or CT can be predictive for the response to various treatments as well as adverse events of adjuvant therapies in OSCC remains unknown.

In conclusion, our data indicated that high densities of CD11b<sup>+</sup> MDSCs in the tumor center or invasive margins significantly correlated with unfavorable survival in patients with primary OSCC. Our findings also suggest that this infiltrating immune subset has pro-tumorigenic effects in OSCC which might be exploited for therapeutic intervention.

## Acknowledgments

This work is financially supported, in whole or in part, by the National Natural Science Foundation of China (81572669, 81602386, 81602378);

Natural Science Foundation of Jiangsu Province (BK20161564, BK20161024); A Project Funded by the Priority Academic Program Development of Jiangsu Higher Education Institutions (2018-87); Project from Nanjing Municipal Committee of Science and Technology (201803044).

Yue Jiang and Chenxing Wang contributed equally to this work.

## Conflict of interest

The authors declare no conflict of interest.

## References

1. Chi AC, Day TA, Neville BW. Oral cavity and oropharyngeal squamous cell carcinoma: an update. *CA Cancer J Clin* 2015; 65: 401-21.
2. O'sullivan B, Brierley J, Byrd D, et al. The TNM classification of malignant tumours – towards common understanding and reasonable expectations. *Lancet Oncol* 2017; 18: 849-51.
3. Okuyemi OT, Piccirillo JF, Spitznagel E. TNM staging compared with a new clinicopathological model in predicting oral tongue squamous cell carcinoma survival. *Head Neck* 2014; 36: 1481-9.
4. Gentles AJ, Newman AM, Liu CL, et al. The prognostic landscape of genes and infiltrating immune cells across human cancers. *Nat Med* 2015; 21: 938-45.
5. Gonzalez H, Hagerling C, Werb Z. Roles of the immune system in cancer: from tumor initiation to metastatic progression. *Genes Dev* 2018; 32: 1267-84.
6. Fridman WH, Pages F, Sautes-Fridman C, Galon J. The immune contexture in human tumours: impact on clinical outcome. *Nat Rev Cancer* 2012; 12: 298-306.
7. Gabrilovich DI. Myeloid-derived suppressor cells. *Cancer Immunol Res* 2017; 5: 3-8.
8. Weide B, Martens A, Zelba H, et al. Myeloid-derived suppressor cells predict survival of patients with advanced melanoma: comparison with regulatory T cells and NY-ESO-1- or melan-A-specific T cells. *Clin Cancer Res* 2014; 20: 1601-9.
9. Wang L, Chang EW, Wong SC, Ong SM, Chong DQ, Ling KL. Increased myeloid-derived suppressor cells in gastric cancer correlate with cancer stage and plasma S100A8/A9 proinflammatory proteins. *J Immunol* 2013; 190: 794-804.
10. Yang G, Shen W, Zhang Y, et al. Accumulation of myeloid-derived suppressor cells (MDSCs) induced by low levels of IL-6 correlates with poor prognosis in bladder cancer. *Oncotarget* 2017; 8: 38378-88.
11. Parker KH, Beury DW, Ostrand-Rosenberg S. Myeloid-derived suppressor cells: critical cells driving immune suppression in the tumor microenvironment. *Adv Cancer Res* 2015; 128: 95-139.
12. Ai L, Mu S, Wang Y, et al. Prognostic role of myeloid-derived suppressor cells in cancers: a systematic review and meta-analysis. *BMC Cancer* 2018; 18: 1220.
13. Deng Y, Cheng J, Fu B, et al. Hepatic carcinoma-associated fibroblasts enhance immune suppression by facilitating the generation of myeloid-derived suppressor cells. *Oncogene* 2017; 36: 1090-101.
14. Edge SB, Byrd DR, Compton CC, Fritz AG, Greene FL, Trotti A. *AJCC Cancer Staging Manual* (7th ed.). Springer, New York 2009.



15. Li Z, Wang Y, Zhu Y, et al. The Hippo transducer TAZ promotes epithelial to mesenchymal transition and cancer stem cell maintenance in oral cancer. *Mol Oncol* 2015; 9: 1091-105.
16. Halama N, Michel S, Kloor M, et al. Localization and density of immune cells in the invasive margin of human colorectal cancer liver metastases are prognostic for response to chemotherapy. *Cancer Res* 2011; 71: 5670-7.
17. Galon J, Pages F, Marincola FM, et al. Cancer classification using the Immunoscore: a worldwide task force. *J Transl Med* 2012; 10: 205.
18. Zhou C, Li J, Wu Y, Diao P, Yang J, Cheng J. High density of intratumor CD45RO(+) memory tumor-infiltrating lymphocytes predicts favorable prognosis in patients with oral squamous cell carcinoma. *J Oral Maxillofac Surg* 2019; 77: 536-45.
19. Zhou C, Wu Y, Jiang L, et al. Density and location of CD3(+) and CD8(+) tumor-infiltrating lymphocytes correlate with prognosis of oral squamous cell carcinoma. *J Oral Pathol Med* 2018; 47: 359-67.
20. Zhou C, Diao P, Wu Y, et al. Development and validation of a seven-immune-feature-based prognostic score for oral squamous cell carcinoma after curative resection. *Int J Cancer* 2020; 146: 1152-63.
21. Camp RL, Dolled-Filhart M, Rimm DL. X-tile: a new bio-informatics tool for biomarker assessment and outcome-based cut-point optimization. *Clin Cancer Res* 2004; 10: 7252-9.
22. Han X, Xu Z, Tian G, et al. Suppression of the long non-coding RNA MALAT-1 impairs the growth and migration of human tongue squamous cell carcinoma SCC4 cells. *Arch Med Sci* 2019; 15: 992-1000.
23. Zhang ST, Wu X, Diao PF, et al. Identification of a prognostic alternative splicing signature in oral squamous cell carcinoma. *J Cell Physiol* 2020; 235: 4804-13.
24. Fletcher M, Ramirez ME, Sierra RA, et al. L-Arginine depletion blunts antitumor T-cell responses by inducing myeloid-derived suppressor cells. *Cancer Res* 2015; 75: 275-83.
25. Hanson EM, Clements VK, Sinha P, Ilkovitch D, Ostland-Rosenberg S. Myeloid-derived suppressor cells down-regulate L-selectin expression on CD4+ and CD8+ T cells. *J Immunol* 2009; 183: 937-44.
26. Serafini P, Mgebroff S, Noonan K, Borrello I. Myeloid-derived suppressor cells promote cross-tolerance in B-cell lymphoma by expanding regulatory T cells. *Cancer Res* 2008; 68: 5439-49.
27. Tartour E, Pere H, Maillere B, et al. Angiogenesis and immunity: a bidirectional link potentially relevant for the monitoring of antiangiogenic therapy and the development of novel therapeutic combination with immunotherapy. *Cancer Metastasis Rev* 2011; 30: 83-95.
28. Shojaei F, Wu X, Qu X, et al. G-CSF-initiated myeloid cell mobilization and angiogenesis mediate tumor refractoriness to anti-VEGF therapy in mouse models. *Proc Natl Acad Sci USA* 2009; 106: 6742-7.
29. Wolf GT, Chepeha DB, Bellile E, Nguyen A, Thomas D, Mchugh J. Tumor infiltrating lymphocytes (TIL) and prognosis in oral cavity squamous carcinoma: a preliminary study. *Oral Oncology* 2015; 51: 90-5.
30. Hu Y, He MY, Zhu LF, et al. Tumor-associated macrophages correlate with the clinicopathological features and poor outcomes via inducing epithelial to mesenchymal transition in oral squamous cell carcinoma. *J Exp Clin Cancer Res* 2016; 35: 12.
31. Singh MM, Johnson B, Venkatarayan A, et al. Preclinical activity of combined HDAC and KDM1A inhibition in glioblastoma. *Neuro Oncol* 2015; 17: 1463-73.
32. Vetsika EK, Koinis F, Gioulbasani M, et al. A circulating subpopulation of monocytic myeloid-derived suppressor cells as an independent prognostic/predictive factor in untreated non-small lung cancer patients. *J Immunol Res* 2014; 2014: 659294.
33. Wu L, Liu H, Guo H, et al. Circulating and tumor-infiltrating myeloid-derived suppressor cells in cervical carcinoma patients. *Oncol Lett* 2018; 15: 9507-15.
34. Pages F, Kirilovsky A, Mlecnik B, et al. In situ cytotoxic and memory T cells predict outcome in patients with early-stage colorectal cancer. *J Clin Oncol* 2009; 27: 5944-51.